

## Measurement of Helicity-Dependent Photoabsorption Cross Sections on the Neutron from 815 to 1825 MeV

H. Dutz,<sup>1</sup> K. Helbing,<sup>2</sup> J. Krimmer,<sup>3,\*</sup> T. Speckner,<sup>2</sup> G. Zeitler,<sup>2</sup> J. Ahrens,<sup>4</sup> S. Altieri,<sup>5,6</sup> J. R. M. Annand,<sup>7</sup> G. Anton,<sup>2</sup> H.-J. Arends,<sup>4</sup> R. Beck,<sup>4</sup> A. Bock,<sup>2</sup> C. Bradtke,<sup>8</sup> A. Braghieri,<sup>5</sup> W. v. Drachenfels,<sup>1</sup> F. Frommberger,<sup>1</sup> M. Godo,<sup>2</sup> S. Goertz,<sup>8</sup> P. Grabmayr,<sup>3</sup> S. Hasegawa,<sup>9</sup> K. Hansen,<sup>10</sup> J. Harmsen,<sup>8</sup> E. Heid,<sup>4</sup> W. Hillert,<sup>1</sup> H. Holvoet,<sup>11</sup> N. Horikawa,<sup>12</sup> T. Iwata,<sup>13</sup> L. Van Hoorebeke,<sup>11</sup> N. d'Hose,<sup>14</sup> P. Jennewein,<sup>4</sup> B. Kiel,<sup>2</sup> F. Klein,<sup>1</sup> R. Kondratiev,<sup>15</sup> M. Lang,<sup>4</sup> B. Lannoy,<sup>11</sup> R. Leukel,<sup>4</sup> V. Lisin,<sup>15</sup> D. Menze,<sup>1</sup> W. Meyer,<sup>8</sup> T. Michel,<sup>2</sup> J. Naumann,<sup>2</sup> A. Panzeri,<sup>5,6</sup> P. Pedroni,<sup>5</sup> T. Pinelli,<sup>5,6</sup> I. Preobrajenski,<sup>4</sup> E. Radtke,<sup>8</sup> G. Reicherz,<sup>8</sup> C. Rohlof,<sup>1</sup> T. Rostomyan,<sup>11</sup> M. Sauer,<sup>3</sup> B. Schoch,<sup>1</sup> M. Schumacher,<sup>16</sup> G. Tamas,<sup>14</sup> A. Thomas,<sup>4</sup> R. van de Vyver,<sup>11</sup> W. Weihofen,<sup>16</sup> and F. Zapadtko<sup>16</sup>

(GDH Collaboration)

<sup>1</sup>Physikalisches Institut, Universität Bonn, D-53115 Bonn, Germany

<sup>2</sup>Physikalisches Institut, Universität Erlangen-Nürnberg, D-91058 Erlangen, Germany

<sup>3</sup>Physikalisches Institut, Universität Tübingen, D-72076 Tübingen, Germany

<sup>4</sup>Institut für Kernphysik, Universität Mainz, D-55099 Mainz, Germany

<sup>5</sup>INFN, Sezione di Pavia, I-27100 Pavia, Italy

<sup>6</sup>Dipartimento di Fisica Nucleare e Teorica, Università di Pavia, I-27100 Pavia, Italy

<sup>7</sup>Department of Physics and Astronomy, University of Glasgow, Glasgow G12 8QQ, United Kingdom

<sup>8</sup>Institut für Experimentalphysik, Ruhr-Universität Bochum, D-44801 Bochum, Germany

<sup>9</sup>Department of Physics, Nagoya University, Chikusa-ku, Nagoya, Japan

<sup>10</sup>MAX-lab, University of Lund, Box 118, S-221 00 Lund, Sweden

<sup>11</sup>Subatomaire en Stralingsfysica, Universiteit Gent, B-9000 Gent, Belgium

<sup>12</sup>CIRSE, Nagoya University, Chikusa-ku, Nagoya, Japan

<sup>13</sup>Department of Physics, Yamagata University, Yamagata, Japan

<sup>14</sup>CEA Saclay, DSM/DAPNIA/SPhN, F-91191 Gif-sur-Yvette Cedex, France

<sup>15</sup>INR, Academy of Science, Moscow, Russia

<sup>16</sup>II. Physikalisches Institut, Universität Göttingen, D-37073 Göttingen, Germany

(Received 15 November 2004; published 28 April 2005)

Helicity-dependent total photoabsorption cross sections on the deuteron have been measured for the first time at ELSA (Bonn) in the photon energy range from 815 to 1825 MeV. Circularly polarized tagged photons impinging on a longitudinally polarized LiD target have been used together with a highly efficient  $4\pi$  detector system. The data around 1 GeV are not compatible with predictions from existing multipole analyses. From the measured energy range an experimental contribution to the GDH integral on the neutron of  $[33.9 \pm 5.5(\text{stat}) \pm 4.5(\text{syst})] \mu\text{b}$  is extracted.

DOI: 10.1103/PhysRevLett.94.162001

PACS numbers: 13.60.Hb, 25.20.Lj

*Introduction.*—A direct experimental verification of the fundamental Gerasimov-Drell-Hearn (GDH) sum rule requires the measurement of photoabsorption cross sections for circularly polarized real photons impinging on longitudinally polarized nucleons. The GDH sum rule reads

$$\int_{\nu_0}^{\infty} \frac{\sigma_{3/2}(\nu) - \sigma_{1/2}(\nu)}{\nu} d\nu = \frac{2\pi^2\alpha}{m^2} \kappa^2. \quad (1)$$

The cross sections  $\sigma_{3/2}$  ( $\sigma_{1/2}$ ) represent a parallel (antiparallel) orientation of photon and nucleon spin in the nucleon rest frame. On the left-hand side, an integration from the pion threshold  $\nu_0$  over the complete excitation spectrum of the nucleon up to infinite high energies  $\nu$  must be performed. The right-hand side includes static nucleon properties like the mass  $m$  and the anomalous magnetic moment  $\kappa$  ( $\alpha$  denotes the electromagnetic fine structure

constant). This sum rule has been derived already in the 1960s [1,2] in a dispersion theoretical approach by the application of fundamental physics principles (Lorentz and gauge invariance, unitarity, causality) only. First measurements on the proton have been completed at the tagged photon facilities of the electron accelerators MAMI [3] and ELSA [4,5] which verify the GDH sum rule for the proton within the statistical limits. In order to check the isospin structure of the sum rule, a measurement on the neutron is necessary. Apart from the sum rule value, knowledge about the energy distribution of the integrand is an important ingredient for the understanding of the nucleon structure.

Prior to doubly polarized experiments, theoretical estimates for  $\Delta\sigma = (\sigma_{3/2} - \sigma_{1/2})$  have been given, which are shown in Fig. 1. In the prediction of the unitary isobar model MAID [6–8] the 3rd resonance region around 1 GeV

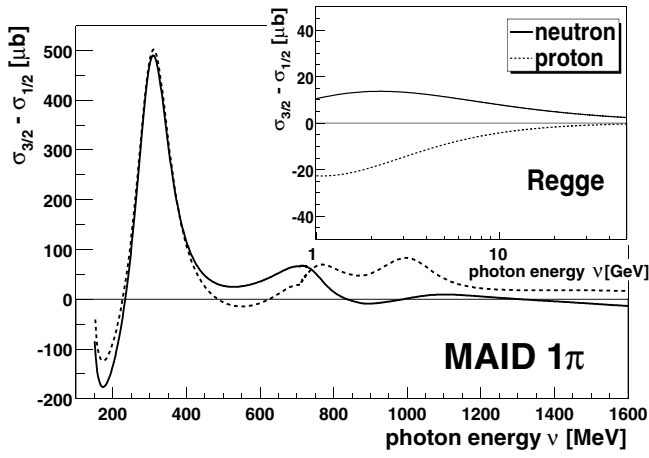


FIG. 1. Predictions for  $\Delta\sigma^n$  (solid lines) and  $\Delta\sigma^p$  (dashed lines) as functions of the photon energy  $\nu$ . Resonance region: one pion contribution from the 2003 solution [6] of MAID [7,8]. High energy behavior (inset) from a Regge approach [9].

on the proton ( $p$ ) is very pronounced, whereas it does not appear for the neutron ( $n$ ). In the  $\Delta$  region the predictions for both nucleons are the same. At higher energies a phenomenological Regge approach [9] predicts  $\Delta\sigma^p$  to be purely negative and  $\Delta\sigma^n$  to be positive over the whole energy range (inset in Fig. 1).

Estimates from multipole analyses for the GDH integral on the neutron  $I_{\text{GDH}}^n = \int_{\nu_{\text{min}}}^{\nu_{\text{max}}} \Delta\sigma^n \frac{d\nu}{\nu}$  are all well below the sum rule value of  $233 \mu\text{b}$  (see, e.g., Ref. [10] and references therein). Possible reasons are an incomplete description of the double pion contribution, improper helicity amplitudes in the 3rd resonance region, and the neglect of the high energy contribution.

In the present experiment only two electron beam energies could be chosen: the first covers the 3rd resonance region, and from the second set the trend of the cross section difference at higher energies can be inferred.

*Experimental setup.*—The experimental setup at ELSA has been described in Ref. [4]. Here, the main aspects are reviewed with emphasis on the measurements with the polarized LiD target.

Circularly polarized tagged photons [11] were produced by bremsstrahlung of longitudinally polarized electrons on thin radiators. Copper foils of  $15 \mu\text{m}$  (Cu15) and  $50 \mu\text{m}$  (Cu50) were used, where the latter was necessary to compensate for a decreased electron beam current. The primary electron energies ( $E_0$ ) 1.2 and 1.9 GeV have been chosen to cover the photon energy range from 815 to 1825 MeV. The electron polarization (40% for 1.2 GeV and 55% for 1.9 GeV at the tagging radiator) was constantly measured via a two-arm Møller polarimeter [12]. The photon polarization  $P_{\text{circ}}(\nu, E_0)$  was determined by the energy dependent helicity transfer [13]. An active collimator system [14] was used to reduce the low energy photon background originating from the collimation process. This device was

also used together with a total absorbing lead glass detector for the determination of the tagging efficiency  $\epsilon_{\text{tag}}(\nu)$  [15]. A photon camera [16] in front of the gamma beam dump monitored the position and intensity of the photon beam and provided feedback to ELSA control. The beam position was stable to better than 0.1 mm during a period of several days [17].

Longitudinally polarized nucleons were provided by a frozen-spin target [18]. The use of a horizontal target cryostat and an internal holding coil [19] allows the detection of emitted particles within nearly  $4\pi$ . The target material  ${}^6\text{LiD}$  contained small admixtures of  ${}^7\text{Li}$  and hydrogen ( $< 5\%$ ) which caused slightly different effective nucleon polarizations  $P_{\text{eff}}^{p,n}$  for the proton and the neutron [19].

$$\begin{aligned}
 P_{\text{eff}}^{p,n} = & a_{6\text{Li}} a_{\text{D}} M_{6\text{LiD}}^{-1} (\alpha_{6\text{Li}}^{p,n} x_{6\text{Li}}^{p,n} P_{6\text{Li}} + \alpha_{\text{D}}^{p,n} x_{\text{D}}^{p,n} P_{\text{D}}) \\
 & + a_{7\text{Li}} a_{\text{D}} M_{7\text{LiD}}^{-1} (\alpha_{7\text{Li}}^{p,n} x_{7\text{Li}}^p P_{7\text{Li}} + \alpha_{\text{D}}^{p,n} x_{\text{D}}^p P_{\text{D}}) \\
 & + a_{6\text{Li}} a_{\text{H}} M_{6\text{LiH}}^{-1} (\alpha_{6\text{Li}}^{p,n} x_{6\text{Li}}^{p,n} P_{6\text{Li}} + \alpha_{\text{H}}^{p,n} x_{\text{H}}^{p,n} P_{\text{H}}) \\
 & + a_{7\text{Li}} a_{\text{H}} M_{7\text{LiH}}^{-1} (\alpha_{7\text{Li}}^{p,n} x_{7\text{Li}}^{p,n} P_{7\text{Li}} + \alpha_{\text{H}}^{p,n} x_{\text{H}}^{p,n} P_{\text{H}}) \quad (2)
 \end{aligned}$$

with  $a_i$  the fraction of the corresponding isotope,  $M_i$  the molar mass,  $\alpha_i$  the number of polarizable nucleons, and  $x_i^{p,n}$  the fraction of nucleons with spins aligned parallel to the nuclear spin. These constants are given in Refs. [19,20]:  $x_{6\text{Li}}^{p,n} = 0.866$  and  $x_{\text{D}}^{p,n} = 0.926$  with uncertainties of 1.4% and 1.7%, respectively. The nuclear polarizations  $P_i$  were derived from the polarization of the free deuteron ( $\approx 29\%$  [19]) by application of the equal spin temperature concept. The area target density  $f_t = \rho l N_A f = (6.970 \pm 0.24) \times 10^{23} \text{ cm}^{-2}$  [19] contains the density  $\rho = 0.820 \text{ g/cm}^3$ , the length of the target cell  $l = (25.90 \pm 0.25) \text{ mm}$ , the Avogadro constant  $N_A$ , and the filling factor  $f = (54.4 \pm 1.6)\%$ .

The GDH detector [21] covers 99.6% of  $4\pi$  with a detection efficiency for charged particles and decay photons of  $\approx 100\%$ . In the forward direction atomic background events (electrons and positrons) were suppressed via a threshold Čerenkov detector [22]. The STAR detector [23] allows for an extrapolation of cross sections to the missing solid angles in forward directions ( $\vartheta < 1.8^\circ$ ).

*Data analysis and systematic errors.*—The principle of the GDH detector is based on the detection of at least one particle produced in a photohadronic reaction while atomic background is rejected.  $\Delta\sigma^{D,n}$  on the deuteron and the neutron have been extracted inclusively according to

$$\begin{aligned}
 \Delta\sigma^{D,n}(\nu) = & \Delta Y^{\text{LiD}}(\nu) \frac{1}{\epsilon_{\text{tag}}(\nu)} \frac{1}{f_t \cdot P_{\text{eff}}^n} \frac{1}{P_{\text{circ}}(\nu, E_0)} \\
 & - \Delta\sigma^p(\nu) g^{D,n}, \quad (3)
 \end{aligned}$$

where the helicity-dependent hadronic count rate  $\Delta Y^{\text{LiD}}(\nu) = N_p^{\text{LiD}} / \phi_p^{\text{el}} - N_a^{\text{LiD}} / \phi_a^{\text{el}}$  is the number of photohadronic events  $N_{p(a)}$  with photon and nuclear spin parallel

TABLE I. The different contributions  $\delta$  to the systematic error of the  $\Delta\sigma$  measurement with the LiD target.

Primary energy $E_0$	1.2 GeV	1.2 GeV	1.9 GeV	
Hadronic rate:	$\delta(\text{energy cuts})$	$\pm 0.7\%$	$\pm 0.7\%$	$\pm 0.7\%$
	$\delta(\text{veto dead time})$	$\pm 0.7\%$	$\pm 0.7\%$	$\pm 0.9\%$
	$\delta(\text{absorption})$	$\pm 0.7\%$	$\pm 0.7\%$	$\pm 0.0\%$
Target:	$\delta(f_i)$	$\pm 3.4\%$	$\pm 3.4\%$	$\pm 3.4\%$
	$\delta(P_{\text{eff}})$	$\pm 2.4\%$	$\pm 2.4\%$	$\pm 2.6\%$
Photons:	Radiator	Cu15	Cu50	Cu15
	$\delta(\epsilon_{\text{tag}})$	$\pm 1.0\%$	$\pm 1.3\%$	$\pm 0.7\%$
	$\delta(P_{\text{circ}})$	$\pm 2.0\%$	$\pm 2.0\%$	$\pm 2.1\%$

or antiparallel, normalized to the incoming electron flux  $\phi_{p(a)}^{\text{el}}$ . This quantity includes the correction due to the veto dead time ( $\approx 20\%$ ) [24]. The factor  $g^D = 0.046$  takes into account the  ${}^7\text{Li}$  and hydrogen contributions to the effective nucleon polarizations [Eq. (2)]. The cross section difference on the proton  $\Delta\sigma^p(\nu)$  has been obtained at the same experimental setup [4,5] with a polarized butanol target.  $\Delta\sigma^n$  can directly be extracted from Eq. (3) with  $g^n = P_{\text{eff}}^p/P_{\text{eff}}^n = 1.045$ . For correct subtraction the raw proton data had been binned according to the LiD data because of different beam energies.

The analysis of the polarized LiD data to obtain  $\Delta\sigma^D$  on the deuteron relies on the cluster assumption of  ${}^6\text{Li}$  being an  $\alpha$  particle and a deuteron. The further decomposition of  $\Delta\sigma^D = \Delta\sigma^p + \Delta\sigma^n$  is based on calculations [25], which show that possible coherent contributions present at lower energies can be neglected here [note that the  $D$ -state probability is taken into account by  $x_i^{p,n}$  in Eq. (2)]. The systematic uncertainty of this model assumption is estimated as  $\delta(\Delta\sigma_{\text{mod}}) = 5\%$  for the neutron.

Control measurements of unpolarized photoabsorption cross sections on beryllium and carbon targets [15,24] are in agreement with literature data [26] and provide an even better statistical precision. The acceptance gap in forward direction has a negligible effect of less than 0.02% on the measured total cross sections [17].

The contributions  $\delta$  to the systematic errors for the measurements of  $\Delta\sigma$  with the LiD target are summarized in Table I. They are similar to the proton ones and are described in Refs. [4,5]. The total systematic error on the neutron  $\delta(\Delta\sigma^n)$  is given by

$$[\delta(\Delta\sigma^n)]^2 = [2\delta(\Delta\sigma_{\text{ind}}^{\text{LiD}})]^2 + [\delta(\Delta\sigma_{\text{ind}}^p)]^2 + [\delta(\Delta\sigma_{\text{corr}})]^2 + [\delta(\Delta\sigma_{\text{mod}})]^2, \quad (4)$$

$\delta(\Delta\sigma_{\text{corr}}) = 2.0\%$  and  $2.3\%$  for  $E_0 = 1.2$  and  $1.9$  GeV, contains the correlated contributions to the systematic error [ $\delta(P_{\text{circ}})$ ,  $\delta(\text{veto dead time})$ ]. The other contributions [ $\delta(\Delta\sigma_{\text{ind}}^{\text{LiD},p})$ ] occur independently for the proton and the LiD target. Just as in [4,5] for each primary energy, no further dependence of the systematic errors on the photon

TABLE II. Helicity-dependent cross section differences for deuteron and neutron, with statistical and systematic errors.

Photon energy $\nu$ (MeV)	Deuteron $\Delta\sigma^D$ ( $\mu\text{b}$ )	Neutron $\Delta\sigma^n$ ( $\mu\text{b}$ )
857	$100.9 \pm 28.9 \pm 4.9$	$61.8 \pm 30.8 \pm 6.8$
943	$137.5 \pm 28.1 \pm 6.7$	$69.2 \pm 29.7 \pm 7.6$
1029	$132.7 \pm 26.5 \pm 6.5$	$46.8 \pm 27.6 \pm 5.2$
1115	$80.0 \pm 27.9 \pm 3.9$	$38.8 \pm 28.8 \pm 4.3$
1313	$41.2 \pm 15.2 \pm 2.0$	$20.1 \pm 16.9 \pm 2.2$
1367	$48.5 \pm 14.4 \pm 2.4$	$31.9 \pm 16.0 \pm 3.4$
1421	$67.4 \pm 14.6 \pm 3.3$	$44.2 \pm 16.1 \pm 4.8$
1475	$44.4 \pm 14.3 \pm 2.2$	$27.2 \pm 15.9 \pm 2.9$
1529	$33.9 \pm 13.7 \pm 1.7$	$11.0 \pm 15.1 \pm 1.2$
1583	$49.7 \pm 13.7 \pm 2.5$	$32.0 \pm 15.1 \pm 3.5$
1637	$33.6 \pm 13.6 \pm 1.7$	$25.6 \pm 14.7 \pm 2.8$
1691	$42.0 \pm 13.4 \pm 2.1$	$31.0 \pm 14.3 \pm 3.3$
1745	$43.1 \pm 13.6 \pm 2.1$	$32.0 \pm 14.5 \pm 3.5$
1799	$49.7 \pm 14.5 \pm 2.5$	$50.8 \pm 15.4 \pm 5.5$

energy is assumed as the rates for the individual tagger channels are similar.

*Results and discussion.*—The results are tabulated in Table II.  $\Delta\sigma^n$  for the neutron is plotted in Fig. 2 as a function of the photon energy in comparison with the proton data from Ref. [5] and theoretical predictions. Even with error bars larger than in the case of the proton, important conclusions can be drawn from the data. The resonance behavior of both nucleons is similar, and even a hint of the 4th resonance region [4] is visible in the neutron case. The proton data cross zero around 2.1 GeV, whereas the neutron shows rather the opposite trend. The neutron data exhibit a structure in the 3rd resonance region around 1 GeV, which is in contradiction to the prediction from [6] (solid line). The data points at higher energies are in

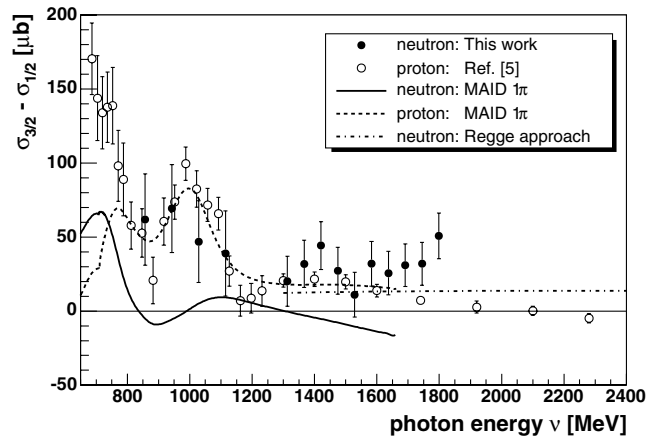


FIG. 2.  $\Delta\sigma^n(\nu)$  in comparison with  $\Delta\sigma^p(\nu)$  [5], theoretical predictions from MAID [6–8] in the resonance region (solid and dashed lines) and a Regge approach for higher energies [9] (dash-dotted line). Error bars are statistical only.

TABLE III. Experimental contributions to  $I_{\text{GDH}}^n$ .

	$\nu$ (MeV)	$I_{\text{GDH}}^n$ ( $\mu\text{b}$ )
ELSA this work	815–1155	$19.8 \pm 5.2 \pm 2.9$
Interpolation	1155–1285	$3.4 \pm 0.5 \pm 0.3$
ELSA this work	1285–1825	$10.7 \pm 1.7 \pm 1.3$

qualitative agreement with the prediction from a phenomenological Regge approach [9].

The experimental contribution to  $I_{\text{GDH}}^n$  from 815 to 1825 MeV is  $[33.9 \pm 5.5(\text{stat}) \pm 4.5(\text{syst})] \mu\text{b}$ . This value includes  $3.4 \mu\text{b}$  from an interpolation between the two data sets (Table III). To allow for an estimation of the GDH integral on the neutron, theoretical predictions for the unmeasured energy ranges have to be taken into account: Below 815 MeV MAID [6,27] gives a theoretical estimate for the single  $\pi$  and  $\eta$ -meson contributions of  $+125$  and  $-2.5 \mu\text{b}$ , respectively. The proton model of [28] has been used for a rough estimate of the double pion contribution on the neutron up to 815 MeV ( $+40 \mu\text{b}$ ). Above 1825 MeV the Regge approach from [9] results in  $+30 \mu\text{b}$ . The sum ( $226 \mu\text{b}$ ) of all experimental and theoretical contributions is, within the experimental error bars, in agreement with the GDH sum rule value ( $233 \mu\text{b}$ ). Note, however, that the present result contributes only 15% to the total value.

Helicity-dependent data on the deuteron from MAMI will be available soon [29] and will provide new input for the multipole analyses used so far in this energy region.

The missing strength of the multipole analyses in the 3rd resonance region requires either a modification of the helicity amplitudes for the  $F_{15}(1680)$  resonance or is caused by an unaccounted double pion contribution. The first possibility is not compatible with differential  $\pi^-$  cross sections [30]. The second case is not favored by the proton data where the strength in the 3rd resonance region seems already exhausted by the single pion contribution (see Fig. 2).

The authors acknowledge the excellent support of the accelerator group of ELSA. This work was supported by the DFG (Germany), the DAAD (Germany), the FWO Vlaanderen (Belgium), the INFN (Italy), the IWT (Belgium), and the Swedish Research Council (Sweden).

\*Corresponding author.

Electronic address: krimmer@pit.physik.uni-tuebingen.de

- [1] S. Gerasimov, Sov. J. Nucl. Phys. **2**, 430 (1966).
- [2] S. Drell and A. Hearn, Phys. Rev. Lett. **16**, 908 (1966).
- [3] J. Ahrens *et al.*, Phys. Rev. Lett. **87**, 022003 (2001).
- [4] H. Dutz *et al.*, Phys. Rev. Lett. **91**, 192001 (2003).
- [5] H. Dutz *et al.*, Phys. Rev. Lett. **93**, 032003 (2004).
- [6] MAID (2003), www.kph.uni-mainz.de/MAID/.
- [7] D. Drechsel, O. Hanstein, S. S. Kamalov, and L. Tiator, Nucl. Phys. **A645**, 145 (1999).
- [8] D. Drechsel, S. S. Kamalov, and L. Tiator, Phys. Rev. D **63**, 114010 (2001).
- [9] N. Bianchi and E. Thomas, Phys. Lett. B **450**, 439 (1999).
- [10] R. A. Arndt, W. J. Briscoe, I. I. Strakovsky, and R. L. Workman, Phys. Rev. C **66**, 055213 (2002).
- [11] J. Naumann *et al.*, Nucl. Instrum. Methods Phys. Res., Sect. A **498**, 211 (2003).
- [12] T. Speckner *et al.*, Nucl. Instrum. Methods Phys. Res., Sect. A **519**, 518 (2004).
- [13] H. Olsen and L. Maximon, Phys. Rev. **114**, 887 (1959).
- [14] G. Zeitler *et al.*, Nucl. Instrum. Methods Phys. Res., Sect. A **459**, 6 (2001).
- [15] G. Zeitler, Ph.D. thesis, Universität Erlangen, Germany, 2002 (to be published).
- [16] J. Krimmer, P. Grabmayr, and M. Sauer, Nucl. Instrum. Methods Phys. Res., Sect. A **481**, 57 (2002).
- [17] J. Krimmer, Ph.D. thesis, Universität Tübingen, Germany, 2004.
- [18] C. Bradtke *et al.*, Nucl. Instrum. Methods Phys. Res., Sect. A **436**, 430 (1999).
- [19] C. Rohlof, Ph.D. thesis, Universität Bonn, Germany, 2003.
- [20] O. A. Rondon, Phys. Rev. C **60**, 035201 (1999).
- [21] K. Helbing *et al.*, Nucl. Instrum. Methods Phys. Res., Sect. A **484**, 129 (2002).
- [22] B. Lannoy, Ph.D. thesis, Universiteit Gent, Belgium, 2000.
- [23] M. Sauer, P. Grabmayr, A. Fuchs, and J. Leypold, Nucl. Instrum. Methods Phys. Res., Sect. A **378**, 143 (1996).
- [24] T. Michel, Ph.D. thesis, Universität Erlangen, Germany, 2001 (to be published).
- [25] A. Fix (private communication); E. Darwish, H. Arenhövel, and M. Schwamb, Eur. Phys. J. A **17**, 513 (2003); H. Arenhövel, A. Fix, and M. Schwamb, Phys. Rev. Lett. **93**, 202301 (2004).
- [26] N. Bianchi *et al.*, Phys. Rev. C **54**, 1688 (1996); V. Muccifora *et al.*, Phys. Rev. C **60**, 64616 (1999); V. Heynen, H. Meyer, B. Naroska, and D. Notz, Phys. Lett. **34B**, 651 (1971).
- [27] W.-T. Chiang, S. N. Yang, L. Tiator, and D. Drechsel, Nucl. Phys. **A700**, 429 (2002).
- [28] H. Holvoet, Ph.D. thesis, Universiteit Gent, Belgium, 2001.
- [29] O. Jahn, Ph.D. thesis, Universität Mainz, Germany (to be published).
- [30] L. Tiator (private communication).